Journal of Bio & Geo Material and Energy (BiGME)
Volume 6 No. 1, February 2026
P-ISSN: 2808-1560 E-ISSN: 2808-1404

Green Synthesis of Iron Oxide Nanoparticles Using Suji Leaf (*Pleomele angustifolia*) Extract Based on Batanghari River Iron Sands

Ade Malemna[1], Lucky Zaehir Maulana[1]*, Frastica Deswardani[1], Rista Mutia Anggraini[1], Febri Berthalita Pujaningsih[1], Muhammad Ficky Afrianto[1], Rozie Sarip[2]

[1]Physics Department, Faculty of Science and Technology, University of Jambi, Jambi, Indonesia
[2]Chemistry Department, Faculty of Science, University of Malaya, Kuala Lumpur, Malaysia

*Email: lucky.maulana@unja.ac.id

Article info:

Submitted: January 2026
Revised: February 2026
Accepted: February 2026
Published: February 2026

Abstract:
Fe_3O_4 nanoparticles were synthesized via a green route using Pleomele angustifolia leaf extract as a bio-reducing and capping agent. XRD analysis confirmed the structure of pure cubic spinel magnetite phase with nanoscale crystallite sizes, while slight lattice variations indicate surface interactions with phytochemicals. SEM images revealed quasi-spherical nanoparticles with average particle sizes of 53–63 nm, where increasing extract concentration reduced agglomeration and improved dispersion. FTIR spectra showed characteristic Fe–O vibrations together with hydroxyl, carbonyl, and aliphatic functional groups, confirming effective surface functionalization by plant-derived compounds. These results demonstrate that Pleomele angustifolia extract regulates nucleation, growth, and surface chemistry during Fe_3O_4 nanoparticle synthesis, highlighting its potential as a sustainable synthesis route for magnetic nanomaterials.

Keywords: Iron oxide, coprecipitation, nanoparticles, green synthesis, *Pleomele angustifolia*

1. Introduction

Industrial growth in Indonesia has expanded significantly in recent years, with the nation currently ranking 38th out of 150 industrialized countries according to the United Nations Industrial Development Organization (UNIDO). However, this rapid development relies heavily on the use of excess chemicals, generating industrial waste that poses a severe threat to the environment if left untreated. Several environmental remediation approaches have been explored to address this wastewater problem, including adsorption (Mehdinia et al., 2019a, 2019b; Ruíz-Baltazar et al., 2015), photocatalysis (Sari et al., 2023; Sudarmono et al., 2024), and electrolysis methods (Pei et al., 2018). These techniques increasingly utilize metal oxides—such as magnetite (Fe_3O_4) derived from iron sand—as a more environmentally friendly alternative for waste treatment.

While conventionally used in various aspects of the construction industry, iron sand has become a focal point for advanced material science. The Jambi province, specifically along the Batanghari River, possesses abundant natural resources of iron sand (Handerson & Sinuraya, 2020). This sand is characterized by its blackish-ash color, indicating a high concentration of iron , making it a highly promising precursor for extracting Fe_3O_4. At the nanoscale, Fe_3O_4 exhibits strong ferromagnetic properties compared to other iron oxides. Consequently, the use of iron sand to produce nano-sized materials is growing rapidly due to its numerous advantages across various industrial applications (Berliana et al., 2025; Liu et al., 2019; Maulana et al., 2013).

Various conventional methods have been employed to synthesize Fe_3O_4 nanoparticles, including hydrothermal, sol-gel, ball-milling, and bottom-up approaches. The chosen synthesis method is critical, as it dictates the resulting particle size, shape, morphology, and crystallinity. Among these, the wet coprecipitation method remains one of the most effective and straightforward techniques. Previous research has successfully utilized coprecipitation to synthesize magnetite nanoparticles from Glagah Beach iron sand, demonstrating

that variations in precipitating agents (like NH_4OH) can effectively tune the crystallite size without altering the fundamental crystal structure or lattice parameters (Fatmawati et al., 2023; Maulana et al., 2013; Prasetyowati et al., 2021; Rahmawati et al., 2018; Salviano et al., 2018; Torkaman et al., 2023).

Despite its efficacy in producing pure Fe_3O_4 nanoparticles, traditional coprecipitation often relies on large quantities of chemical precursors, rendering the process less eco-friendly. To mitigate this, recent studies have pivoted towards "green synthesis," an approach that utilizes natural organic materials from plants or microorganisms as alternative reducing agents. Plant extracts contain secondary metabolites—such as flavonoids, alkaloids, and chlorophyll—that act as excellent bioreductors and capping agents. This sustainable method has been successfully demonstrated using various botanical sources, including mimba leaves, shallot skin, and betel leaves (Aryani & Wisnuwardhani, 2022; Ashutosh Kumar Shukla & Siavash Iravani, 2018; Astuti, khaira, et al., 2022; Bassim et al., 2022; Cuana et al., 2022; Melvin et al., 2020; Parvathi et al., 2023; Rahayuningsih et al., 2018; Syihabuddin & Munasir, 2024; Yoga Darmawan et al., 2023).

In this study, we aim to synthesize magnetic nanoparticles from Batanghari River iron sand using Suji leaves (Pleomele angustifolia) as a novel bio-reducing agent. Suji leaf extract was selected because its primary constituents are highly suitable for green synthesis ; it is rich in flavonoids, alkaloids, triterpenoids, glycosides, and chlorophyll. The high concentration of flavonoids and chlorophyll inherently serves as a powerful antioxidant and capping agent during nanoparticle formation. By varying the concentration of the Suji leaf extract, this study investigates its regulatory effect on the resulting crystal size. The synthesized nanoparticles were systematically characterized using X-Ray Diffraction (XRD), Scanning Electron Microscopy (SEM), and Fourier Transform Infrared (FTIR) spectroscopy.

2. Material and Method

Material

The iron sands in this study have been collected from the Batanghari River, Jambi Province. The type of sand taken is sand that has a mostly black colour that indicated the high contains of Fe element. HCl, $FeCl_3$, $FeCl_2$, Fe_2O_3 and NH_4OH were analytical grade from Mercks.

Preparation of sand

The sand that has been collected was dried for approximately two days using sun light after washed by distilled water at least 3 times. The dried sand was sieved to obtain a uniform size. The iron sands are extracted using a permanent magnet to separate the sands that high amount of Fe inside. The sand was subsequently ground with a mortar and pestle and sieved through a 120-mesh sieve to produce finer, more uniformly sized particles.

Preparation of Suji leaf extracts

The next important step is preparing Suji leaf extract. This stage has been done by cutting Suji leaves in 1 cm^2 size leaves. The dried leaves then mashed until we got a powder. Then extraction of Suji leaves has been done by maceration method. The process is started by dissolving 400 grams of Suji leaf powder with 1 L 96% ethanol. The solution was then stirred with a hot plate stirrer for 30 minutes and allowed to stand for 24 hours at room temperature with a glass jar covered using black plastic. The extraction process was carried out for 3 days with solvent replacement every day. The extract was then separated from the solvent using a rotary evaporator at 40°C until the extract thickened.

Preparation of nanoparticles iron oxide

A total of 40 grams of iron sand was dissolved with 38 ml of HCl (12M) in a beaker and stirred for about 60 minutes using a magnetic stirrer at 55°C. The use of HCl aims to dissolve iron sand and help accelerate the reaction process in the formation of $FeCl_3$, $FeCl_2$ and Fe_2O_3. The process can be seen in the equation below:

$$3Fe_3O_{4(s)} + 8HCl_{(l)} \longrightarrow 2FeCl_{3(l)} + 3Fe_2O_{(s)} + 3H_2O_{(1)} + H_{2(g} \quad (1)$$

$$2FeCl_{3(1)} + FeCl_{2(1)} + H_2O_{(1)} + 8NH_4OH_{(1)} \rightarrow Fe_3O_{4(S)} + 8NH_4Cl_{(1)} + 5H_2O_{(1)} \quad (2)$$

For the Fe_3O_4 nanoparticles green synthesis, we add Suji leaf extract. The filtrate that has been obtained, then added with 15 mL of Suji leaf extract with several variations of Suji leaf extract. Here, we use

concentrations of 33.3%, 66.7% and 100% with distilled water as the solvent. Then stirred again for 15 minutes at 60ºC. After that, 73 mL NH_4OH was added drop by drop to the previous solution for 30 minutes at 60ºC. Then allowed to stand for 60 minutes until a precipitate was obtained. The precipitate was then washed using distilled water for 7 times until the Ph is 7 using Ph meter. Then the precipitate was dried in an oven for 2 hours until we got iron oxide nanoparticles (Astuti et al., 2022; Liu et al., 2019; Mehdinia et al., 2020; Novita & Astuti, 2023). In this paper we named Fe_3O_4 as the sample that has been prepared by conventional wet coprecipitation methods and GS1, GS2 and GS3 as the sample that has been prepared by green synthesize route as seen in Table1. The iron oxide that mainly composed of Fe_3O_4 then investigated by XRD, SEM and FTIR characterization. The nanoparticles were characterized by FTIR to analyse the functional groups that present in the samples. XRD characterization was carried out to determine the crystal structure, lattice parameters and crystallite size of the samples and SEM was used to grasp the morphology and average particle size.

Table 1. Sample Name

Sample Name	Iron sand (g)	Extract Concentration from 15 ml green agent addition
Fe_3O_4	40	0.0 %
GS1	40	33.3%
GS2	40	66.7%
GS3	40	100%

3. Results and Discussion

The extraction of Iron oxide sand from the river sands produced 24% iron oxide. In our experiment, we obtained nanoparticles of iron oxide using conventional methods as much as 6.82 grams, while in the green synthesis way, we obtained in average of 4.85 grams of nanoparticles.

X-ray diffraction (XRD) analysis was employed to investigate the crystalline structure of Fe_3O_4 and the Fe_3O_4 from green synthesis named GS1, GS2, and GS3. As seen in Figure 1, the diffraction pattern of Fe_3O_4 exhibits distinct reflections at 2θ values of approximately 30.1°, 35.4°, 43.1°, 57.0°, and 62.6°, which can be indexed to the (220), (311), (400), (511), and (440) planes of cubic spinel magnetite, respectively. These peaks are in good agreement with the standard JCPDS card No. 19-0629, confirming the formation of single-phase Fe_3O_4 with an inverse spinel structure (space group Fd–3m) (Astuti et al., 2022; Begum et al., 2025; Gatta et al., 2007; Husain et al., 2019; Liu et al., 2019; Mehdinia et al., 2020; Novita & Astuti, 2023).

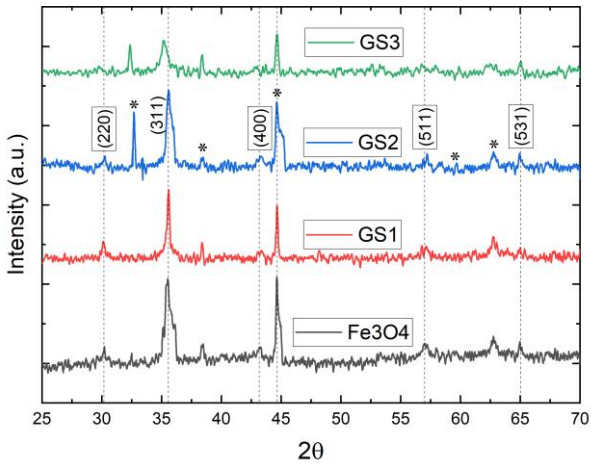

Figure 1. XRD patterns of iron oxide nanoparticles magnetite with and hematite* impurities, synthesized by conventional wet methods route (black) and green synthesized with various *Pleomele angustifolia* extract.

The most intense diffraction peak observed at ~35.4°, corresponding to the (311) plane, is characteristic of magnetite and indicates good crystallinity of the Fe_3O_4 phase. For the GS1, GS2, and GS3 samples, all major Fe_3O_4 diffraction peaks are retained without any noticeable shift in peak positions, suggesting that the incorporation of green agent extract does not alter the crystal structure or lattice parameters of Fe_3O_4.

A gradual decrease in the relative intensity of the Fe_3O_4 peaks is observed with increasing Suji leaf extract content, which can be attributed to the partial coverage of Fe_3O_4 particles by the green extract and the reduced effective diffracting volume. Additional weak diffraction peaks marked with asterisks originate from the GS component, which is predominantly amorphous or poorly crystalline. Notably, no impurity phases such as α-Fe_2O_3 or γ-Fe_2O_3 are detected, indicating that Fe_3O_4 remains structurally stable during Suji leaf extract addition.

Table 2. 2θ, lattice parameter and crystal size at peak (311) of pure Fe_3O_4; Fe_3O_4 + 33.3% *Pleomele angustifolia* (GS1); Fe_3O_4 + 66.7% *Pleomele angustifolia* (GS2); and Fe_3O_4 + 100% *Pleomele angustifolia* (GS3).

Sample name	d_{311} at 35.4 ° (Å)	Lattice Parameter (Å)	Crystallite Size (nm)
Fe_3O_4	2.527	8.381	12.44
GS1	2.520	8.357	31.81
GS2	2.521	8.361	19.20
GS3	2.544	8.439	14.52

The structural parameters of Fe_3O_4 and GS1, GS2, and GS3 samples were evaluated from the dominant (311) diffraction peak at $2\theta \approx 35.4°$, and the results are summarized in Table 2. The interplanar spacing (*d*) was calculated using Bragg's law:

$$d = \frac{\lambda}{2\sin\theta}$$

where λ is the wavelength of Cu Kα radiation (1.5406 Å) and θ is the Bragg angle. For pristine Fe_3O_4, the calculated d_{311} value is 2.527 Å, which closely matches the standard magnetite value reported in JCPDS No. 19-0629, confirming the formation of phase-pure cubic Fe_3O_4(El-Desoky et al., 2020; Wardani et al., 2019).

The lattice parameter (a) for the cubic system was calculated using the relation:

$$a = d\sqrt{h^2 + k^2 + l^2}$$

The lattice parameter of Fe_3O_4 was determined to be 8.381 Å, which is in good agreement with the reported bulk value (~8.39 Å). For GS1 and GS2, slight reductions in *d*-spacing (2.520 and 2.521 Å) and lattice parameter (8.357 and 8.361 Å, respectively) are observed, indicating lattice contraction due to interfacial strain and surface effects at the nanoscale. In contrast, GS3 exhibits an increased d-spacing of 2.544 Å and an expanded lattice parameter of 8.439 Å, which may be attributed to lattice relaxation, defect formation, or strain release induced by higher green content.

The crystallite size (*D*) was estimated using the Scherrer equation:

$$D = \frac{0.9\lambda}{\beta\cos\theta}$$

where β is the full width at half maximum (FWHM) of the diffraction peak (in radians). The crystallite size of pristine Fe_3O_4 is 12.44 nm, whereas GS1 shows a significantly larger size of 31.81 nm, suggesting enhanced crystallinity or reduced microstrain. With further GS incorporation, the crystallite size decreases to 19.20 nm (GS2) and 14.52 nm (GS3), likely due to growth inhibition and confinement effects. These results demonstrate that GS modulates the microstructural properties of Fe_3O_4 without altering its cubic spinel phase (El-Desoky et al., 2020; Kittel, 2004; Wardani et al., 2019).

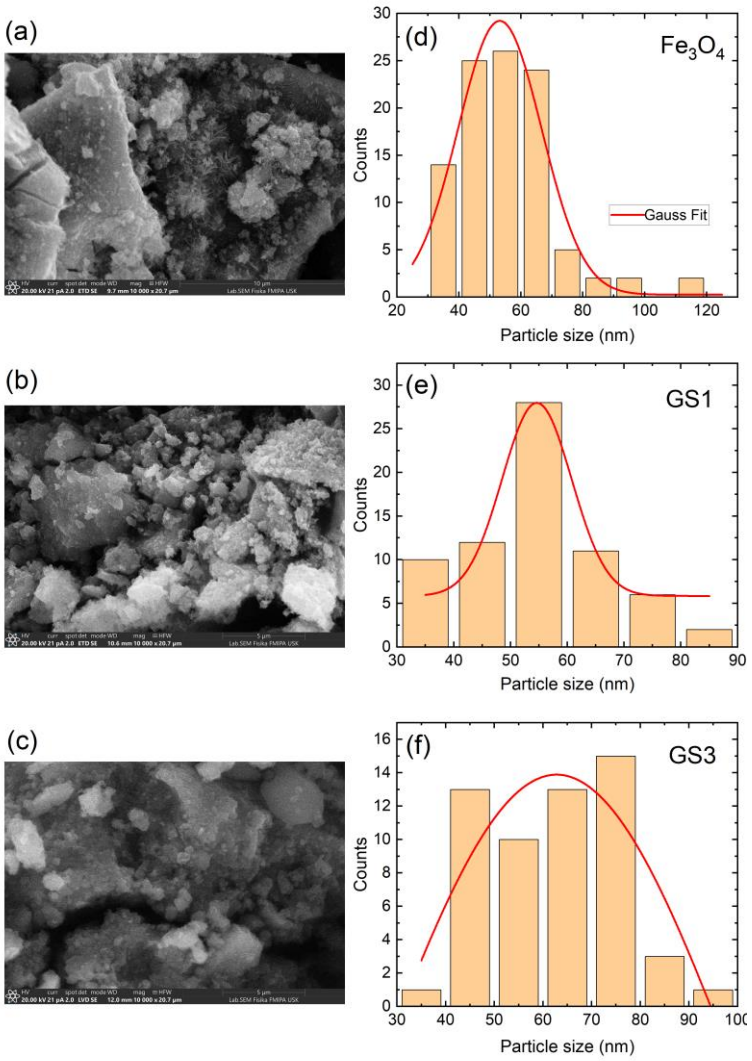

Figure 2. SEM of a) Fe_3O_4 , b) GS1 and c) GS3 and their respected particle size distribution

SEM was used to examine the morphology and particle size distribution of Fe_3O_4 and GS-based composites (Fig. 2). Particle size distributions were extracted from SEM images using ImageJ and fitted with Gaussian functions in Origin Pro (see Figure 2(d–f)). Fe_3O_4 (Figure 2(a)) consists of agglomerated, quasi-spherical nanoparticles, which is typical for magnetite due to magnetic interactions. The particle size distribution (Fig. 2(d)) shows an average particle size of 53 ± 1.2 nm, which is larger than the crystallite size obtained from XRD, indicating polycrystalline particles.

A critical observation in this study is the marked difference between the crystallite sizes obtained via XRD (12.44 – 31.81 nm) and the physical particle sizes observed via SEM (53 – 63 nm). It is imperative to distinguish between these two metrics. The Scherrer equation applied to XRD data measures the crystallite size, defined as the size of a single, coherently scattering crystalline domain. Conversely, SEM measures the morphological particle size, which represents the outer physical boundary of the material.

The fact that the SEM particle sizes are significantly larger than the XRD crystallite sizes indicates that the observed Fe_3O_4 nanoparticles are highly polycrystalline. In other words, each physical nanoparticle observed under the electron microscope is an agglomeration of multiple, smaller single-crystal domains. This agglomeration is a common phenomenon in magnetic nanomaterials, driven by strong magnetic dipole-dipole interactions between the Fe_3O_4 cores, as well as high surface-to-volume ratios that thermodynamically favor clustering to minimize surface energy. The addition of the Pleomele angustifolia extract clearly modulates this

behavior; while it successfully acts as a surface passivating agent to improve dispersion at optimal concentrations (GS1) , the fundamental polycrystalline nature of the nanoparticles remains.

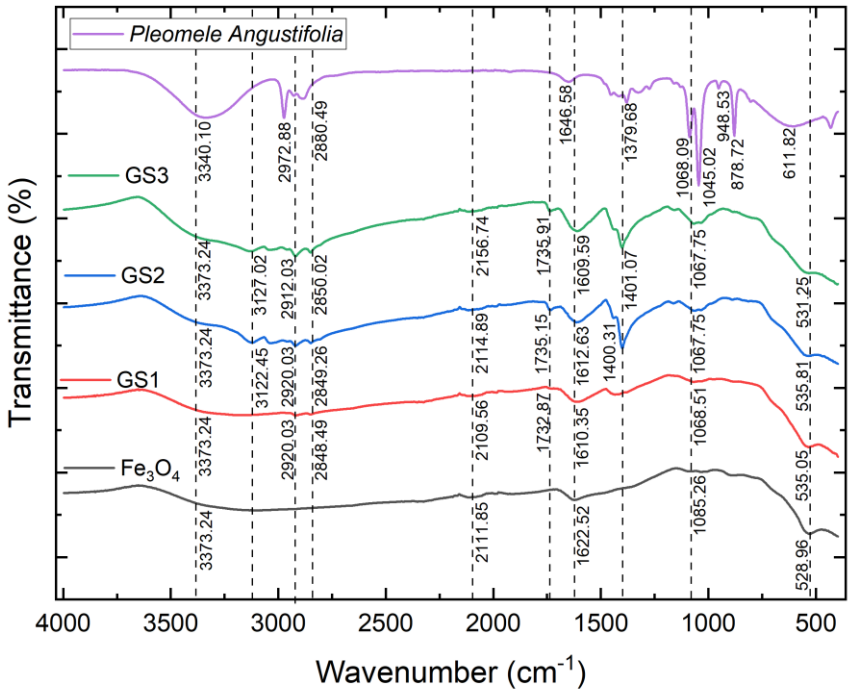

Figure 3. Form up to bottom: FTIR spectra of Suji Leaf, GS3, GS2, GS1 and Fe_3O_4.

Figure 3 presents the FTIR spectra of pristine Fe_3O_4, Fe_3O_4 synthesized with different concentrations of *Pleomele angustifolia* (Suji leaf) extract (GS1, GS2, and GS3), and the pure Suji leaf extract. The presence of a strong absorption band in the low-wavenumber region (~528–536 cm^{-1}) in all samples is attributed to the Fe–O stretching vibration, which is characteristic of magnetite nanoparticles and confirms the successful formation of Fe_3O_4 in all synthesis conditions (Panda et al., 2021). For Fe_3O_4, the Fe–O vibration appears at 528.96 cm^{-1}, while a systematic shift toward higher wavenumbers is observed upon the addition of Suji leaf extract, appearing at 535.05 cm^{-1} (GS1), 535.81 cm^{-1} (GS2), and 535.25 cm^{-1} (GS3). This shift indicates strong interfacial interactions between Fe_3O_4 nanoparticles and phytochemical compounds present in the extract, suggesting effective surface modification and stabilization of the nanoparticles (Khatun et al., 2022; Rahmayanti et al., 2022).

The appearance of new absorption bands in the regions 2848–2850 cm^{-1} and ~2920 cm^{-1} in the GS samples corresponds to C–H stretching vibrations of aliphatic groups, which originate from organic compounds in the suji leaf extract. These bands are absent or significantly weaker in Fe_3O_4, confirming the incorporation of plant-derived biomolecules on the nanoparticle surface. Broad absorption bands observed in the range ~3120–3340 cm^{-1} are assigned to O–H stretching vibrations, which arise from hydroxyl groups of phenolic compounds in the extract as well as adsorbed water molecules forming hydrogen bonds. The increasing intensity of these bands with higher extract concentration indicates enhanced surface hydroxylation and stronger hydrogen-bond interactions.

The absorption bands appearing in the region ~1609–1735 cm^{-1} are attributed to C=O stretching vibrations of carbonyl-containing functional groups such as ketones, esters, and carboxylic acids. These functional groups play a crucial role as capping and stabilizing agents, preventing nanoparticle agglomeration during synthesis (Astuti, khaira, et al., 2022; Novita & Astuti, 2023; Parmita et al., 2023). The persistence and shift of these bands across GS1–GS3 samples confirm the successful adsorption of organic compounds from the suji leaf extract onto the Fe_3O_4 surface. In the GS2 sample, an additional absorption band observed around ~1401 cm^{-1} is assigned to C–N stretching vibrations, which are associated with nitrogen-containing compounds such as chlorophyll present in the suji leaf extract. The intensity and position of this band shift with increasing extract concentration, further confirming the role of phytochemicals in surface

functionalization. For the GS3 sample (100% extract), a noticeable decrease in the intensity of the Fe–O band is observed, which may be attributed to excessive organic coverage on the Fe_3O_4 surface. Additionally, the C–O stretching vibration observed at ~1067.75 cm^{-1} and the intensified aromatic C–H bands indicate a higher organic content at the nanoparticle surface, consistent with increased extract concentration.

Overall, the FTIR results confirm the presence of Fe_3O_4 in all samples and demonstrate that *Pleomele angustifolia* leaf extract acts effectively as a reducing, capping, and stabilizing agent during nanoparticle synthesis. The coexistence of Fe–O vibrations and multiple organic functional groups provides strong evidence for the successful formation of Fe_3O_4/biomolecule composites.

4. Conclusion

sustainable green route utilizing Pleomele angustifolia (Suji leaf) extract as a bio-reducing and capping agent. X-ray diffraction (XRD) analysis confirmed the formation of a phase-pure cubic spinel structure with nanoscale crystallite dimensions, where slight variations in lattice parameters indicated surface modifications induced by phytochemical adsorption. Scanning Electron Microscopy (SEM) revealed quasi-spherical particles, demonstrating that the addition of the extract effectively suppressed agglomeration and improved particle dispersion through surface passivation at optimal concentrations. Furthermore, FTIR spectroscopy corroborated these structural findings by identifying characteristic Fe–O vibrations alongside key organic functional groups such as hydroxyls, carbonyls, and aliphatic chains, evidencing strong interfacial interactions between the magnetite surfaces and the plant-derived biomolecules. Ultimately, these findings demonstrate that plant-derived biomolecules play a crucial role in regulating surface chemistry, particle growth, and stability, presenting a promising and sustainable pathway for the development of surface-engineered magnetic nanomaterials.

References

Aryani, A. D., & Wisnuwardhani, H. A. (2022). Studi Literatur Sintesis Nanopartikel Tembaga Menggunakan Bioreduktor Ekstrak Tumbuhan dengan Aktivitas Antioksidan. *Jurnal Riset Farmasi*, 41–48. https://doi.org/10.29313/JRF.V2I1.843

Astuti, A., khaira, ihda, Arief, syukri, & Usna, S. R. A. (2022). Sintesis dan Karakterisasi Struktur dan Sifat Magnet Nanokomposit Fe_3O_4@PEG:ZnO. *Indonesian Journal of Applied Physics*, *12*(2), 217–224. https://doi.org/10.13057/IJAP.V12I2.58514

Astuti, Khaira, I., Arief, S., & Usna, S. R. A. (2022). Sintesis dan Karakterisasi Struktur dan Sifat Magnet Nanokomposit Fe_3O_4@PEG:ZnO. *Indonesian Journal of Applied Physics*, *12*(2), 217. https://doi.org/10.13057/ijap.v12i2.58514

Bassim, S., Mageed, A. K., AbdulRazak, A. A., & Majdi, H. S. (2022). Green Synthesis of Fe_3O_4 Nanoparticles and Its Applications in Wastewater Treatment. *Inorganics*, *10*(12). https://doi.org/10.3390/inorganics10120260

Begum, S. K., Shabnam, D., Haque, N., Alam, M. J., Ferdous, J., Nur, U. J. B., Fatema, K., Shabiha, R. J., Clarke, R. J., Chowdhury, P., & Uddin, M. N. (2025). Green synthesis of magnetite (Fe_3O_4) and hematite (Fe2O3) nanoparticles using Moringa oleifera and Psidium guajava leaf extracts for sustainable applications. *Scientific Reports 2025 15:1*, *15*(1), 36465-. https://doi.org/10.1038/s41598-025-21603-4

Berliana, A. P., Deswardani, F., Pujaningsih, F., Anggraini, R. M., & Maulana, L. Z. (2025). Analisis Variasi Konsentrasi Ekstrak Daun Pandan (Pandanus Amaryllifolius) pada Green Synthesis Nanopartikel Magnetit (Fe_3O_4) Berbasis Pasir Besi (Iron Sands) Sungai Batang Hari. *Journal Online of Physics*, *10*(3), 126–134. https://doi.org/10.22437/JOP.V10I3.46458

Cuana, R., Panre, A. M., Istiqomah, N. I., Tumbelaka, R. M., Sunaryono, S., Wicaksono, S. T., & Suharyadi, E. (2022). Green Synthesis of Fe3O4/Chitosan Nanoparticles Utilizing Moringa Oleifera Extracts and Their Surface Plasmon Resonance Propertie. *ECS Journal of Solid State Science and Technology*, *11*(8), 11. https://doi.org/10.1149/2162-8777/AC8B36

El-Desoky, H. S., Khalifa, A., & Abdel-Galeil, M. M. (2020). An advanced and Facile Synthesized Graphene/Magnetic Fe 3 O 4 Nanoparticles Platform for Subnanomolar Voltammetric Determination of Antipsychotic Olanzapine Drug in Human Plasma . *Journal of The Electrochemical Society*, *167*(6). https://doi.org/10.1149/1945-7111/ab8366

Fatmawati, T., Shiddiq, M., Armynah, B., & Tahir, D. (2023). Synthesis Methods of Fe3O4 Nanoparticles for Biomedical Applications. In *Chemical Engineering and Technology* (Vol. 46, Number 11). https://doi.org/10.1002/ceat.202200384

Gatta, G. D., Kantor, I., Boffa Ballaran, T., Dubrovinsky, L., & McCammon, C. (2007). Effect of non-hydrostatic conditions on the elastic behaviour of magnetite: An in situ single-crystal X-ray diffraction study. *Physics and Chemistry of Minerals*, *34*(9), 627–635. https://doi.org/10.1007/S00269-007-0177-3/METRICS

Handerson, W., & Sinuraya, S. (2020). Analisa Sifat Magnetik dan Identifikasi Kandungan Pasir Sungai Kampar Provinsi Riau. *Komunikasi Fisika Indonesia*, *17*(2), 92. https://doi.org/10.31258/jkfi.17.2.92-96

Husain, S., Hadi Haryanti, N., Novalina Manik, T., Monica Hutasoit, S., Riyanto, A., Yani KM, J. A., Selatan Program Studi Kimia, K., Lambung Mangkurat, U., Selatan Program Studi Fisika, K., Lampung Jl Sumantri Brojonegoro No, U., & Lampung, B. (2019). Potensi Nanokomposit Fe_3O_4@C dari Bijih Besi Sebagai Pendeteksi Kadar Glukosa. *POSITRON*, *9*(2), 44–52. https://doi.org/10.26418/POSITRON.V9I2.32771

Khatun, R., Mamun, M. S. Al, Islam, S., Khatun, N., Hakim, M., Hossain, M. S., Dhar, P. K., & Barai, H. R. (2022). Phytochemical-Assisted Synthesis of Fe_3O_4 Nanoparticles and Evaluation of Their Catalytic Activity. *Micromachines*, *13*(12). https://doi.org/10.3390/mi13122077

Kittel, C. (2004). Introduction to Solid State Physics, 8th edition. *Wiley & Sons, New York, NY*.

Liu, K., Qin, Y., Muhammad, Y., Zhu, Y., Tang, R., Chen, N., Shi, H., Zhang, H., Tong, Z., & Yu, B. (2019). Effect of Fe_3O_4 content and microwave reaction time on the properties of Fe_3O_4/ZnO magnetic nanoparticles. *Journal of Alloys and Compounds*, *781*. https://doi.org/10.1016/j.jallcom.2018.12.085

Maulana, L. Z., Yulianto, A., & Sulhadi. (2013). Aplikasi low density polyethylene (LDPE) pada pembuatan magnet ferrite komposit. *Jurnal Sains Dasar*, *2*(1), 72–78. https://doi.org/10.21831/JSD.V2I1.3571

Mehdinia, A., Hazrati, N., & Mozaffari, S. (2020). Synthesis and characterization of Fe_3O_4@polythionine-Au for the removal and pre-concentration of Cu(II) from marine samples. *Journal of the Iranian Chemical Society*, *17*(12), 3327–3338. https://doi.org/10.1007/S13738-020-01989-W/METRICS

Mehdinia, A., Mirzaeipour, R., & Jabbari, A. (2019a). Nanosized Fe3O4–curcumin conjugates for adsorption of heavy metals from seawater samples. *Journal of the Iranian Chemical Society*, *16*(7), 1431–1439. https://doi.org/10.1007/S13738-019-01619-0/METRICS

Mehdinia, A., Mirzaeipour, R., & Jabbari, A. (2019b). Nanosized Fe_3O_4–curcumin conjugates for adsorption of heavy metals from seawater samples. *Journal of the Iranian Chemical Society*, *16*(7), 1431–1439. https://doi.org/10.1007/S13738-019-01619-0/METRICS

Melvin, M., Bakri, R., & Yulizar, Y. (2020). Green synthesis of gold nanoparticles supported in Al-pillared bentonite using aqueous leaf extracts of Dracaena angustifolia and their use for reductive degradation of methyl orange. *Journal of Physics: Conference Series*, *1442*(1). https://doi.org/10.1088/1742-6596/1442/1/012060

Novita, D., & Astuti, A. (2023). Sintesis dan Karakterisasi Sifat Optik Nanokomposit Fe_3O_4@CQD (Carbon Quantum Dots). *Jurnal Fisika Unand*, *12*(2), 311–316. https://doi.org/10.25077/JFU.12.2.310-315.2023

Panda, S. K., Aggarwal, I., Kumar, H., Prasad, L., Kumar, A., Sharma, A., Vo, D. V. N., Van Thuan, D., & Mishra, V. (2021). Magnetite nanoparticles as sorbents for dye removal: a review. *Environmental Chemistry Letters 2021 19:3*, *19*(3), 2487–2525. https://doi.org/10.1007/S10311-020-01173-9

Parmita, A. W. Y. P., Panji, Dewanto, H. A., Sasongko, A., Qulub, F., Triana, Y., & Parmita, A. W. Y. P. (2023). Studi Pengaruh Temperatur Kalsinasi dalam Pembentukan Nanomagnetit dengan Metode Green Synthesis Ekstrak Daun Nanas. *SPECTA Journal of Technology*, *7*(2), 584–592. https://doi.org/10.35718/SPECTA.V7I2.940

Parvathi, E., Akshaya, C. V., Dilraj, N., Arjun, G., & Deepak, N. K. (2023). Green synthesis of reduced graphene oxide by shallots. *Materials Today: Proceedings*. https://doi.org/10.1016/j.matpr.2023.04.309

Pei, S., Wei, Q., Huang, K., Cheng, H. M., & Ren, W. (2018). Green synthesis of graphene oxide by seconds timescale water electrolytic oxidation. *Nature Communications*, *9*(1). https://doi.org/10.1038/s41467-017-02479-z

Prasetyowati, R., Widiawati, D., Swastika, P. E., Ariswan, A., & Warsono, W. (2021). Sintesis dan Karakterisasi Nanopartikel Magnetit (Fe_3O_4) Berbasis Pasir Besi Pantai Glagah Kulon Progo dengan

Metode Kopresipitasi pada Berbagai Variasi Konsentrasi NH4OH. *Jurnal Sains Dasar*, *10*(2), 57–61. https://doi.org/10.21831/JSD.V10I2.43043

Rahayuningsih, E., Pamungkas, M. S., Olvianas, M., & Putera, A. D. P. (2018). Chlorophyll extraction from suji leaf (Pleomele angustifolia Roxb.) with ZnCl2 stabilizer. *Journal of Food Science and Technology*, *55*(3). https://doi.org/10.1007/s13197-017-3016-7

Rahmawati, R., Taufiq, A., Sunaryono, S., Fuad, A., Yuliarto, B., Suyatman, S., & Kurniadi, D. (2018). Synthesis of Magnetite (Fe_3O_4) Nanoparticles from Iron sands by Coprecipitation-Ultrasonic Irradiation Methods. *Journal of Materials and Environmental Science*, *9*(1). https://doi.org/10.26872/jmes.2018.9.1.19

Rahmayanti, M., Yahdiyani, A., & Afifah, I. Q. (2022). Eco-friendly synthesis of magnetite based on tea dregs (Fe_3O_4-TD) for methylene blue adsorbent from simulation waste. *Communications in Science and Technology*, *7*(2). https://doi.org/10.21924/cst.7.2.2022.965

Ruíz-Baltazar, A., Pérez, R., Ruíz-Baltazar, A., & Pérez, R. (2015). Kinetic Adsorption Study of Silver Nanoparticles on Natural Zeolite: Experimental and Theoretical Models. *Applied Sciences 2015, Vol. 5, Pages 1869-1881*, *5*(4), 1869–1881. https://doi.org/10.3390/APP5041869

Salviano, L. B., Silva Cardoso, T. M. da, Silva, G. C., Silva Dantas, M. S., & Mello Ferreira, A. de. (2018). Microstructural Assessment of Magnetite Nanoparticles (Fe_3O_4) Obtained by Chemical Precipitation Under Different Synthesis Conditions. *Materials Research*, *21*(2), e20170764. https://doi.org/10.1590/1980-5373-MR-2017-0764

Sari, E. K., Tumbelaka, R. M., Ardiyanti, H., Istiqomah, N. I., Chotimah, & Suharyadi, E. (2023). Green synthesis of magnetically separable and reusable Fe_3O_4/Cdots nanocomposites photocatalyst utilizing Moringa oleifera extract and watermelon peel for rapid dye degradation. *Carbon Resources Conversion*, *6*(4), 274–286. https://doi.org/10.1016/J.CRCON.2023.04.003

Sudarmono, Istiqomah, N. I., Budianti, S. I., Cuana, R., Puspitarum, D. L., Mahardhika, L. J., Chotimah, & Suharyadi, E. (2024). Magnetically separable and reusable Fe_3O_4/chitosan nanocomposites green synthesized utilizing Moringa oleifera extract for rapid photocatalytic degradation of methylene blue. *Results in Chemistry*, *7*. https://doi.org/10.1016/j.rechem.2023.101245

Syihabuddin, D. M., & Munasir, M. (2024). Green Synthesis Nanopartikel Fe_3O_4 Dengan Bioreduktor Ekstrak Daun Mimba (Azadirachta Indica): Aplikasi Sebagai Material Fotokatalis Degradasi Methylene Blue. *Inovasi Fisika Indonesia*, *13*(3), 118–123. https://doi.org/10.26740/IFI.V13N3.P118-123

Torkaman, P., Karimzadeh, R., & Jafari, A. (2023). Assessment of the synthesis method of Fe_3O_4 nanocatalysts and its effectiveness in viscosity reduction and heavy oil upgrading. *Scientific Reports*, *13*(1). https://doi.org/10.1038/s41598-023-41441-6

Wardani, R. K., Dahlan, K., Wahyudi, S. T., & Sukaryo, S. G. (2019). Synthesis and characterization of nanoparticle magnetite for biomedical application. *AIP Conference Proceedings*, *2194*. https://doi.org/10.1063/1.5139869

Yoga Darmawan, M., Imani Istiqomah, N., Adrianto, N., Marsel Tumbelaka, R., Dwi Nugraheni, A., & Suharyadi, E. (2023). Green synthesis of Fe_3O_4/Ag composite nanoparticles using Moringa oleifera: Exploring microstructure, optical, and magnetic properties for magnetic hyperthermia applications. *Results in Chemistry*, *6*, 100999. https://doi.org/10.1016/J.RECHEM.2023.100999